ELSEVIER

Journal of Molecular Structure: THEOCHEM 716 (2005) 193–198

THEO CHEM

www.elsevier.com/locate/theochem

Prediction of high weight polymers glass transition temperature using RBF neural networks

Antreas Afantitis, Georgia Melagraki, Kalliopi Makridima, Alex Alexandridis, Haralambos Sarimveis*, Olga Iglessi-Markopoulou

School of Chemical Engineering, National Technical University of Athens, 9, Heroon Polytechniou Str., Zografou Campus, Athens 15780, Greece

Received 9 September 2004; accepted 4 November 2004
Available online 5 January 2005

Abstract

A novel approach to the prediction of the glass transition temperature (T_g) for high molecular polymers is presented. A new quantitative structure–property relationship (QSPR) model is obtained using Radial Basis Function (RBF) neural networks and a set of four-parameter descriptors, $\sum \mathrm{MV}_{(\mathrm{ter})}(R_{\mathrm{ter}})$, L_F, ΔX_{SB} and $\sum \mathrm{PEI}$. The produced QSPR model ($R^2=0.9269$) proved to be considerably more accurate compared to a multiple linear regression model ($R^2=0.8227$).

Keywords: RBF neural network; QSPR; Glass transition temperature

1. Introduction

Determination of the physical properties of organic compounds based on their structure is a major research subject in computational chemistry. Quantitative structure–property relationship (QSPR) correlations have been widely applied for the prediction of such properties over the last decades [1–3]. A breakthrough has occurred in this field with the appearance of artificial neural networks (ANNs).

The glass transition is the most important transition and relaxation that occurs in amorphous polymers. It has a significant effect on the properties and processing characteristics of this type of polymers [4]. The glass transition (T_g) is difficult to be determined because the transition happens over a comparatively wide temperature range and depends on the method, the duration and the pressure of the measuring device [5,6]. Besides these difficulties, the experiments are costly and time consuming.

In the past, numerous attempts have been made to predict T_g for polymers by different approaches. According to Katrinzky et al. [7] there are two kinds of approaches, the empirical and the theoretical. Empirical methods correlate the target property with other physical or chemical properties of the polymers, for example, group additive properties (GAP) [8]. The most widely referenced model of the theoretical estimations produced by Bicerano [6] combines a weighted sum of structural parameters along with the solubility parameter of each polymer. In his work, a regression model was produced for 320 polymers but no external data set compounds were used to validate this model.

Cameilio et al. [9] calculated the parameters of 50 acrylates and methylacrylates with molecular mechanics and correlated them with T_g. Katrizky et al. [10] introduced a model for 22 medium molecular weight polymers using four parameters. Following this work, Katrinzky et al. [7] and Cao and Lin [11] obtained two separate models for 88 un-cross-linked homopolymers including polyethylenes, polyacrylates, polymethylacrylates, polystyrenes, polyethers, and polyoxides. The models were used as predictors of the molar glass transition temperatures [7] (T_g/M) and glass transition temperatures [11]. Joyce et al. [12] used neural networks for the prediction of T_g based on monomer structure of polymers. Another approach with neural network was proposed by Sumpter and Noid [13] using

* Corresponding author. Tel.: +30 210 772 3237; fax: +30 210 772 3138.
E-mail address: hsarimv@central.ntua.gr (H. Sarimveis).

0166-1280/$ - see front matter © 2004 Elsevier B.V. All rights reserved.
doi:10.1016/j.theochem.2004.11.021

the repeating unit structure as representative of the polymer. Finally Jurs and Mattioni [14] obtained a QSPR model which predicts T_g values for a diverse set of polymers.

An ANN-based modeling method could produce a more accurate QSPR model compared to linear methods, since it has the ability to approximate the possible non-linear relationships between structural information and properties of compounds during the training process. The resulting model can generalize the knowledge among homologous series without need for theoretical formulas [6]. In this work we explore these neural network capabilities, by introducing a new QSPR model for the prediction of T_g values that is based on the RBF architecture. The database consists of 88 un-cross-linked homopolymers and contains the experimental values of T_g and the values of the following descriptors $\sum \mathrm{MV}_{(\mathrm{ter})}(R_{\mathrm{ter}})$, L_F, ΔX_{SB} and $\sum \mathrm{PEI}$. All the data are taken from Cao and Lin [11].

2. Modeling methodology

In this section we present the basic characteristics of the RBF neural network architecture and the training method that was used to develop the QSAR neural network models.

2.1. RBF network topology and node characteristics

RBF networks consist of three layers: the input layer, the hidden layer and the output layer. The input layer collects the input information and formulates the input vector $\mathbf{x}$. The hidden layer consists of L hidden nodes, which apply non-linear transformations to the input vector. The output layer delivers the neural network responses to the environment. A typical hidden node l in an RBF network is described by a vector $\hat{\mathbf{x}}_l$, equal in dimension to the input vector and a scalar width σ_l. The activity $v_l(\mathbf{x})$ of the node is calculated as the Euclidean norm of the difference between the input vector and the node center and is given by:

$$v_l(\mathbf{x}) = \|\mathbf{x} - \hat{\mathbf{x}}_l\| \tag{1}$$

The response of the hidden node is determined by passing the activity through the radially symmetric Gaussian function:

$$f_l(\mathbf{x}) = \exp\left(-\frac{v_l(\mathbf{x})^2}{\sigma_l^2}\right) \tag{2}$$

Finally, the output values of the network are computed as linear combinations of the hidden layer responses:

$$\hat{y}_m = g_m(\mathbf{x}) = \sum_{l=1}^{L} f_l(\mathbf{x}) w_{l,m}, \quad m = 1, \ldots, M \tag{3}$$

where $[w_{1,m}, w_{2,m}, \ldots, w_{L,m}]$ is the vector of weights, which multiply the hidden node responses in order to calculate the mth output of the network.

2.2. RBF network training methodology

Training methodologies for the RBF network architecture are based on a set of input–output training pairs ($\mathbf{x}(k)$; $\mathbf{y}(k)$) ($k = 1,2,\ldots,K$). The training procedure used in this work consists of three distinct phases:

(i) Selection of the network structure and calculation of the hidden node centers using the fuzzy means clustering algorithm [15]. The algorithm is based on a fuzzy partition of the input space, which is produced by defining a number of triangular fuzzy sets on the domain of each input variable. The centers of these fuzzy sets produce a multidimensional grid on the input space. A rigorous selection algorithm chooses the most appropriate knots of the grid, which are used as hidden node centers in the produced RBF network model. The idea behind the selection algorithm is to place the centers in the multidimensional input space, so that there is a minimum distance between the center locations. At the same time the algorithm assures that for any input example in the training set, there is at least one selected hidden node that is close enough according to a distance criterion. It must be emphasized that opposed to both the k-means [16] and the c-means clustering [17] algorithms, the fuzzy means technique does not need the number of clusters to be fixed before the execution of the method. Moreover, due to the fact that it is a one-pass algorithm, it is extremely fast even if a large database of input–output examples is available.

(ii) Following the determination of the hidden node centers, the widths of the Gaussian activation function are calculated using the p-nearest neighbour heuristic [18]

$$\sigma_l = \left(\frac{1}{p}\sum_{i=1}^{p} \|\hat{\mathbf{x}}_l - \hat{\mathbf{x}}_i\|^2\right)^{1/2} \tag{4}$$

where $\hat{\mathbf{x}}_1, \hat{\mathbf{x}}_2, \ldots, \hat{\mathbf{x}}_p$ are the p nearest node centers to the hidden node l. The parameter p is selected, so that many nodes are activated when an input vector is presented to the neural network model.

(iii) The connection weights are determined using linear regression between the hidden layer responses and the corresponding output training set.

3. Results and discussion

The data set of 88 polymers was divided into a training set of 44 polymers, and a validation set of 40 polymers, while 4 polymers were rejected as outliers. The selection of the compounds in the training set was made according to the structure of the polymers, so that representatives of a wide range of structures (in terms of the different branching

and length of the carbon chain) were included. The polymers in the training set and validation sets along with the collected from the literature [11] experimental glass transition temperatures are presented in Tables 1 and 2, respectively.

Structural parameters for the 84 polymers were calculated by the equations provided in the literature [11]. Two sets of descriptors were formulated. The first one (set 1) includes four parameters $\sum MV_{(ter)}(R_{ter})$, L_F, ΔX_{SB} and $\sum PEI$, while the second one (set 2) incorporates only three parameters $\sum MV_{(ter)}(R_{ter})$, $\sum PEI$ and ΔX_{SB}. ΔX_{SB} is related to the polarity of the repeating unit, while dipole of the side group depends on $\sum PEI$ [11]. These two parameters express the intermolecular forces of the polymers. $\sum MV_{(ter)}(R_{ter})$ expresses the no free rotation part of the side chain and L_F (free length) expresses the bond count of the free rotation part of side chain [11]. The four descriptors are very attractive because they can be calculated easily, rapidly and they have clear physical meanings.

The RBF training method described in Section 2 was implemented using the Matlab computing language in order to produce the ANN models. It should be emphasized that the method has been developed in-house, so no commercial packages were utilized to build the neural network models. For comparison purposes, a standard multivariate regression

Table 1
Training set

A/A	Name	$T_{g(K),exp}$ [7]	$T_{g(K),train\ (set\ 1\ ANN)}$, $R^2=0.9968$	$T_{g(K),train\ (set\ 2\ ANN)}$, $R^2=0.9699$	$T_{g(K),train\ (set\ 1\ linear)}$, $R^2=0.9305$	$T_{g(K),train\ (set\ 2\ linear)}$, $R^2=0.7978$
1	Poly(ethylene)	195	198.5551	198.5575	206.2141	180.7988
2	Poly(butylethylene)	220	218.7587	221.2788	235.0911	232.7334
3	Poly(cyclohexylethylene)	363	366.3575	358.4639	344.6778	325.4238
4	Poly(methyl acrylate)	281	281.7356	283.8484	275.8405	266.8474
5	Poly(*sec*-butyl acrylate)	253	253.3203	230.8956	253.2285	253.0170
6	Poly(vinyl chloride)	348	347.5609	350.5647	342.3186	313.8412
7	Poly(vinyl acetate)	301	300.9527	302.0354	301.0322	292.5775
8	Poly(2-chrolostyrene)	392	387.1948	389.7748	365.8097	348.3518
9	Poly(4-chrolostyrene)	389	384.5742	386.5308	365.7563	348.7295
10	Poly(3-methylstyrene)	374	373.9529	374.5706	364.4905	348.2874
11	Poly(4-fluorostyrene)	379	388.5550	385.5003	362.0613	343.8790
12	Poly(1-pentene)	220	221.4911	215.7971	244.9158	232.5792
13	Poly(*tert*-butyl acrylate)	315	313.5255	315.9148	320.2125	321.7363
14	Poly(vinyl hexyl ether)	209	204.7662	205.8718	207.1528	243.3611
15	Poly(1,1-dichloroethylene)	256	256.2872	256.2894	247.1680	193.4119
16	Poly(a-methylstyrene)	409	408.4218	391.5212	401.2537	376.0410
17	Poly(ethyl methylacrylate)	324	325.1226	333.8064	316.7212	312.6020
18	Poly(ethyl chloroacrylate)	366	365.1200	348.3090	369.4096	365.8042
19	Poly(*tert*-butyl methylacrylate)	380	380.6744	355.6613	392.4762	392.3873
20	Poly(chlorotrifluoroethylene)	373	372.8955	369.6086	370.0549	335.4887
21	Poly(oxyethylene)	206	198.5551	198.5575	206.2141	180.7988
22	Poly(oxytetramethylene)	190	198.5551	198.5575	206.2141	180.7988
23	Poly(vinyl-*n*-octyl ether)	194	195.1257	202.8784	185.9801	242.6692
24	Poly(oxyoctamethylene)	203	198.5551	198.5575	206.2141	180.7988
25	Poly(vinyl-*n*-pentyl ether)	207	213.3238	208.3135	217.8674	243.8824
26	Poly(*n*-octyl acrylate)	208	208.4627	220.8631	187.1082	248.5577
27	Poly(*n*-heptyl acrylate)	213	210.4768	221.5301	198.0531	249.2561
28	Poly(*n*-hexyl acrylate)	216	218.3827	222.6153	209.1625	250.1351
29	Poly(vinyl-*n*-butyl ether)	221	216.9422	211.9548	228.7795	244.6534
30	Poly(vinylisobutyl ether)	251	252.1121	251.0763	289.1591	292.7876
31	Poly(pentafluoroethyl ethylene)	314	314.6488	321.3212	333.3871	324.1696
32	Poly(3,3-dimethylbutyl methacrylate)	318	317.5529	359.6010	365.0133	385.2956
33	Poly(vinyl trifluoroacetate)	319	319.0651	318.1759	304.0800	311.4646
34	Poly(*n*-butyl a-chloroacrylate)	330	329.7446	348.2495	350.1299	366.8521
35	Poly(heptafluoropropyl ethylene)	331	330.5015	322.4316	322.2799	322.6774
36	Poly(5-methyl-1-hexene)	259	267.9876	281.9314	285.4562	280.9634
37	Poly(*n*-hexyl methacrylate)	268	268.3445	263.7424	266.4187	302.5932
38	Poly[*p*-(*n*-butyl)styrene]	279	278.0939	273.3399	250.3024	247.1930
39	Poly(2-methoxyethyl methacrylate)	293	292.1270	289.0940	278.0316	307.6720
40	Poly(4-methyl-1-pentene)	302	291.4458	281.6227	295.7158	280.9432
41	Poly(*n*-propyl methacrylate)	306	304.5211	304.7446	302.5679	308.3655
42	Poly(3-phenyl-1-propene)	333	333.0387	333.3597	319.1753	309.1556
43	Poly(*sec*-butyl a-chloroacrylate)	347	348.2163	348.9745	360.7427	366.9406
44	Poly(vinyl acetal)	355	354.5809	354.8202	356.0620	353.4776

Table 2
Validation set

A/A	Name	$T_{g(K),exp}$ [7]	$T_{g(K),pred\ (set\ 1\ ANN)}$, $R^2=0.9269$	$T_{g(K),pred\ (set\ 2\ ANN)}$, $R^2=0.9252$	$T_{g(K),pred\ (set\ 1\ linear)}$, $R^2=0.8227$	$T_{g(K),pred\ (set\ 2\ linear)}$, $R^2=0.7097$
1	Poly(ethylethylene)	228	225.7773	206.1942	254.3056	232.2911
2	Poly(cyclopentylethylene)	348	358.7344	343.5276	333.7406	312.7605
3	Poly(acrylic acid)	379	370.7699	383.7025	329.0515	303.8972
4	Poly(ethyl acrylate)	251	260.9209	246.7095	258.6331	259.2738
5	Poly(acrylonitrile)	378	345.0173	371.8758	313.8227	286.6382
6	Poly(styrene)	373	371.7688	347.9344	346.6853	326.8437
7	Poly(3-chrolostyrene)	363	384.5075	389.0822	368.3181	351.7191
8	Poly(4-methylstyrene)	374	374.1514	372.7100	361.5876	344.9300
9	Poly(propylene)	233	226.4469	187.9298	262.2846	231.5684
10	Poly(ethoxyethylene)	254	225.3849	228.6502	252.0064	247.9495
11	Poly(*n*-butyl acrylate)	219	245.6944	227.1540	232.2903	252.9285
12	Poly(1,1-difluoroethylene)	233	195.4623	198.3722	216.6780	184.0215
13	Poly(methyl methylacrylate)	378	353.2666	381.0222	334.3601	320.6272
14	Poly(isopropyl methylacrylate)	327	346.2991	335.9038	340.3382	329.0090
15	Poly(2-chloroethyl methyl acrylate)	365	320.4176	374.1077	308.9656	314.1617
16	Poly(phenyl methylacrylate)	393	384.4661	383.4895	389.6478	387.7161
17	Poly(oxymethylene)	218	198.5551	198.5575	206.2141	180.7988
18	Poly(oxytrimethylene)	195	198.5551	198.5575	206.2141	180.7988
19	Poly(vinyl-*n*-decyl ether)	197	193.8290	194.0785	154.2539	230.9803
20	Poly(oxyhexamethylene)	204	198.5551	198.5575	206.2141	180.7988
21	Poly(vinyl-2-ethylhexyl ether)	207	203.3388	200.5523	207.2539	243.0972
22	Poly(*n*-octyl methylacrylate)	253	231.6752	251.2710	244.1416	300.7819
23	Poly(*n*-nonyl acrylate)	216	205.7941	220.5435	176.3024	248.0084
24	Poly(1-heptene)	220	215.2582	224.7551	225.0757	232.8289
25	Poly(*n*-propyl acrylate)	229	254.0266	233.0850	244.7675	255.3384
26	Poly(vinyl-*sec*-butyl ether)	253	212.4641	205.6889	239.7295	244.8458
27	Poly(2,3,3,3-tetrafluoropropylene)	315	302.9461	313.9999	376.8912	360.9749
28	Poly(*N*-butyl acrylamide)	319	287.7707	290.2156	292.0473	307.4908
29	Poly(3-methyl-1-butene)	323	315.5115	283.7897	306.5165	281.0895
30	Poly(*sec*-butyl methacrylate)	330	299.0857	283.5890	300.4798	305.8099
31	Poly(3-pentyl acrylate)	257	251.1566	230.2371	241.6161	251.4401
32	Poly(oxy-2,2-dichloromethyl trimethylene)	265	262.6800	250.3470	239.6464	195.2553
33	Poly(vinyl isopropyl ether)	270	270.4936	252.7574	300.6332	294.0386
34	Poly(*n*-butyl methacrylate)	293	290.0164	285.9807	289.8661	305.7211
35	Poly(3,3,3-trifluoropropylene)	300	271.9207	316.5163	345.6684	327.9476
36	Poly(vinyl chloroacetate)	304	298.8250	345.7275	265.9810	272.7775
37	Poly(3-cyclopentyl-1-propene)	333	337.5040	338.5281	321.8972	312.2930
38	Poly(*n*-propyl a-chloroacrylate)	344	351.9808	348.1715	359.9544	366.4854
39	Poly(3-cyclohexyl-1-propene)	348	348.9284	351.6250	332.4757	324.8458
40	Poly(vinyl formal)	378	372.8332	369.3446	377.9002	366.2196

Table 3
Summary of the results produced by the different methods

	Parameters	Method	Training set	Validation set	R^2_{train}	R^2_{pred}	Figure	Equation
1	Set 1	Neural network	44	40	0.9968	0.9269	1	–
2	Set 2	Neural network	44	40	0.9699	0.9252	2	–
3	Set 1	Linear	44	40	0.9305	0.8227	3	5
4	Set 2	Linear	44	40	0.7978	0.7097	4	6
5	Set 1	Cross-validation, neural network	84-i	i	–	0.9269	5	–
6	Set 2	Cross-validation, neural network	84-i	i	–	0.8501	–	–
7	Set 1	Cross-validation, linear	84-i	i	–	0.8719	6	–
8	Set 2	Cross-validation, linear	84-i	i	–	0.7253	–	–

method for producing linear models was also utilized. Both neural networks and linear models were trained using the 44 individuals in the training set and were tested on the independent validation set consisting of 40 examples. The models produced by multiple linear regression on the two sets of descriptors are shown next:

$$T_g\,(\mathrm{K}) = 0.3617\sum \mathrm{MV}_{ter}(R_{ter}) - 10.3254L_F + 159.7984\Delta X_{SB} + 9.3931\Sigma\mathrm{PEI} + 206.2141 \quad (5)$$

$$T_g\,(\mathrm{K}) = 0.4394\sum \mathrm{MV}_{ter}(R_{ter}) + 167.2681\Delta X_{SB} + 2.8929\Sigma\mathrm{PEI} + 180.7988 \quad (6)$$

The RBF models generated using the two sets of descriptors consisted of 34 and 25 hidden nodes, respectively. RBF models are more complex compared to the linear models and are not shown in the paper for brevity, but can be available to the interested reader. The produced ANN QSPR models for the prediction of glass transition temperature, proved to be more accurate compared to multiple linear regression models using both sets of descriptors as shown in Table 3, where the results are summarized. More detailed results can be found in Tables 1 and 2 where the estimations of the two modeling techniques for the training examples and the predictions for the validation examples are depicted in an example-to-example basis. There are four columns of results in the two tables corresponding to the two modeling methodologies and the two sets of descriptors. Figs. 1–4 show the experimental glass transition temperatures vs. the predictions produced by the neural network and the multiple regression techniques in a graphical representation format.

To further explore the reliability of the proposed method we also used the leave-one-out cross-validation method on the full set of the available data (excluding the outliers). The results are summarized in Table 3 and are shown in

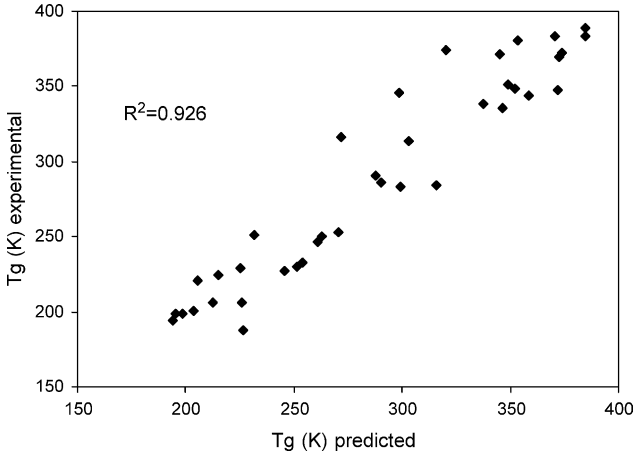

Fig. 1. Experimental vs predicted T_g for 40 polymers (set 1 ANN).

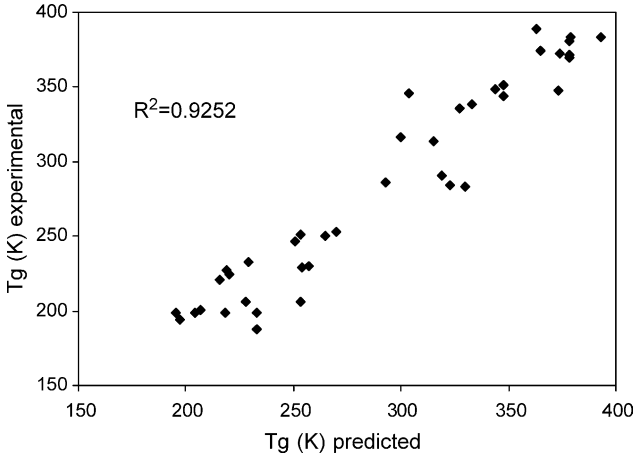

Fig. 2. Experimental vs predicted T_g for 40 polymers (set 2 ANN).

Figs. 5 and 6, where again the superiority of the neural network methodology over the multiple linear regression method is clear. It should be mentioned, that contrary to the aforementioned results, there is a decrease in the R^2 statistic in both modeling methodologies when the three-descriptor set is utilized. However, the R^2 statistic for the neural network methodology using the second set of descriptors is still high, meaning that the respective neural network model is reliable.

Summarizing the results presented in this work we can make the following observations:

(i) The modeling procedures utilized in this work (separation of the data into two independent sets and leave-one-out cross-validation) illustrated the accuracy of the produced models not only by calculating their fitness on sets of training data, but also by testing the predicting abilities of the models.

(ii) We showed that using the neural network methodology we can still have a reliable prediction, when the descriptor L_F is dropped. Therefore, a three-descriptor ANN model can be used for the prediction of the glass transition temperature at

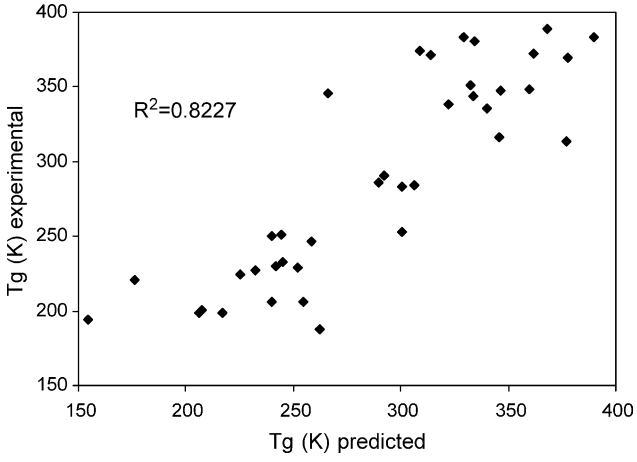

Fig. 3. Experimental vs predicted T_g for 40 polymers (set 1 linear).

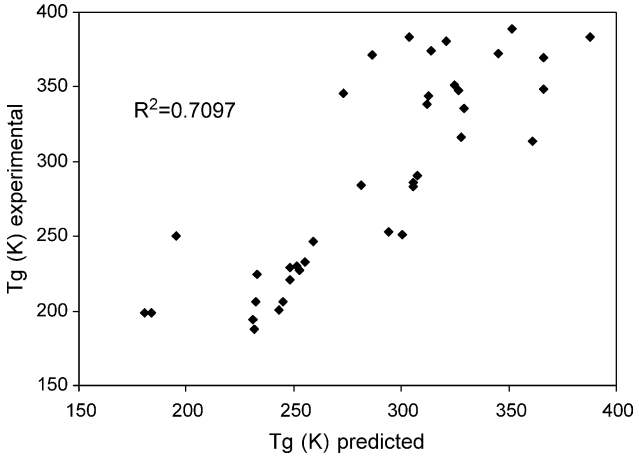

Fig. 4. Experimental vs predicted T_g for 40 polymers (set 2 linear).

the expense of the increased complexity of the model compared to the simple structure of a linear model.

4. Conclusions

The results of this study show that a practical model can be constructed based on the RBF neural network architecture for a set of 84 high molecular weight polymers. The most accurate models were generated using four descriptors and resulted in the following statistics: $R^2_{\text{set 1}} = 0.9968$ for the training data, $R^2_{\text{set 1}} = 0.9269$ for the validation data and $R^2_{\text{set 1,CV}} = 0.9269$ for the cross-validation method. We showed that using the neural network approach, we can further reduce the number of descriptors from four to three and still produce a reliable model. The neural network models are produced based on the special fuzzy means training method for RBF networks that exhibits small computational times and excellent prediction accuracies. The proposed method could be a substitute to the costly and time-consuming experiments for determining glass

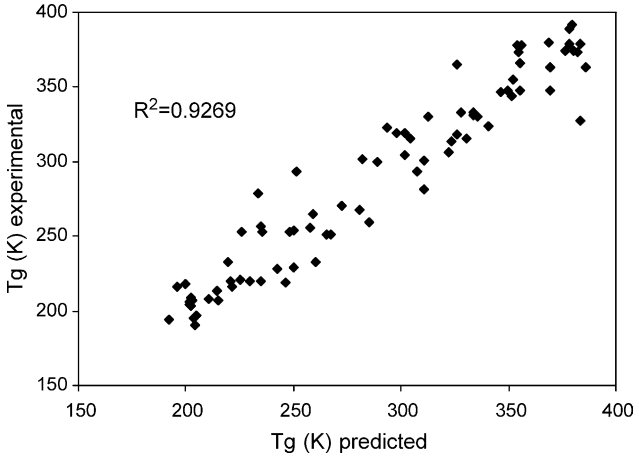

Fig. 5. Experimental vs predicted T_g with cross-validation (set 1 ANN).

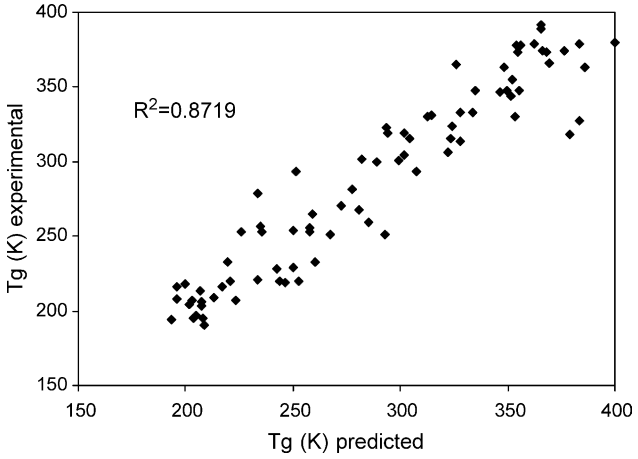

Fig. 6. Experimental vs predicted T_g with cross-validation (set 1 linear).

transition temperatures or to the approximate empirical equations with limited reliability.

Acknowledgments

A. Af. wishes to thank the A.G. Leventis Foundation for its financial support.

References

[1] I. Gutman, S.J. Cyvin, Introduction to the Theory of Benzenoid Hydrocarbons, Springer, Berlin, 1989.
[2] P.V. Khadikar, S. Karmarkar, V.K. Agrawal, Natl Acad. Sci. Lett. 23 (2000) 23.
[3] R.F. Rekker, R. Mannhold, Calculation of Drug Lipophilicity, Wiley, New York, 1992.
[4] J. Bicerano, The Dow Chemical Company, Midland, Michigan, Encyclopedia of Polymer Science and Technology, Wiley, New York, 2003.
[5] S. Krause, J.J. Gormley, N. Roman, J.A. Shetter, W.H. Watanade, J. Polym. Sci.: Part A 3 (1965) 3573.
[6] J. Bicerano, Prediction of Polymers Properties, second ed., Marcel Dekker, New York, 1996.
[7] A.R. Katrinzky, S. Sild, V. Lobanov, M.J. Karelson, J. Chem. Inf. Comput. Sci. 38 (1998) 300.
[8] D.W. Van Krevelen, Properties of Polymers. Their Estimation and Correlation with Chemical Structure, second ed., Elsevier, Amsterdam, 1976.
[9] P. Cameilio, V. Lazzeri, B. Waegell, Polym. Preprints: Am. Chem. Soc. Div. Polym. Chem. 36 (1995) 661.
[10] A.R. Katrizky, P. Rachwal, K.W. Law, M. Karelson, V.S. Lobanov, J. Chem. Inf. Comput. Sci. 36 (1996) 879.
[11] C. Cao, Y. Lin, J. Chem. Inf. Comput. Sci. 43 (2003) 643.
[12] S.J. Joyce, D.J. Osguthorpe, J.A. Padgett, G.J. Price, J. Chem. Soc. Faraday Trans. 91 (1995) 2491.
[13] B.G. Sumpter, D.W. Noid, J. Thermal Anal. 46 (1996) 833.
[14] B.E. Mattioni, P.C. Jurs, J. Chem. Inf. Comput. Sci. 42 (2002) 232.
[15] H. Sarimveis, A. Alexandridis, G. Tsekouras, G. Bafas, Ind. Eng. Chem. Res. 41 (2002) 751.
[16] C. Darken, J. Moody, 2 (1990) 233.
[17] J.C. Dunn, J. Cybernet 3 (1973) 32.
[18] J.A. Leonard, M.A. Kramer, IEEE Control Syst. 31 (1991).